ELSEVIER

Thermochimica Acta 290 (1997) 173–180

thermochimica acta

Eutectic mixtures for pharmaceutical applications: A thermodynamic and kinetic study

Narcís Clavaguera[a,*], Joan Saurina[b], Jean Lheritier[c], Jacqueline Masse[c], Alain Chauvet[c], Maria Teresa Clavaguera-Mora[d]

[a] *Grup de Física de l'Estat Sòlid, Departament d'Estructura i Constituents de la Matèria, Facultat de Física, Universitat de Barcelona, Barcelona, 08028, Spain*

[b] *Departament de Física, Universitat de Girona, Girona, Spain*

[c] *Laboratoire de Chimie Générale et Minérale, Faculté de Pharmacie, Université de Montpellier I, Montpellier, France*

[d] *Grup de Física de Materials I, Departament de Física, Universitat Autònoma de Barcelona, Bellaterra 08193, Spain*

Received 25 May 1996; revised 3 July 1996; accepted 12 July 1996

Abstract

The thermodynamics and kinetics of the solidification process of several mixtures of SR 33557 and PEG 6000 have been analyzed by differential scanning calorimetry. The calculated phase diagram showed a negative interaction energy between the constituents in the liquid phase. A unified description for solidification accounting for isothermal and continuous cooling is presented. The onset of solidification shifts to higher temperatures on decreasing the cooling rate and to longer times on decreasing the annealing temperature under continuous cooling and isothermal holding, respectively. The analysis is based on the fact that nuclei have to be created prior to any crystal growth. The driving force for nucleation is considered proportional to the undercooling, $\Delta T(=T_L - T)$. By coupling the isothermal and continuous cooling experiments, the high temperature part of the time–temperature transformation and temperature–cooling rate transformation diagrams are constructed under a wide range of conditions. © 1997 Elsevier Science B.V.

Keywords: Activation energy; Nucleation; PEG-mixtures; Polyethylene glycol; Temperature–cooling rate transformation curves; Time–temperature transformation curves

1. Introduction

The knowledge of the phase diagram of a drug and an excipient is of major interest in pharmaceutical technology. In particular, the phase diagram of SR 33557 and polyethylene glycol with mean molecular weight between 5400 and 6000 (PEG 6000) has been previously reported [1]. The drug SR 33557 (CAS 114432-13-2) was developed by SANOFI-Recherche [2,3] with a general formula $C_{31}H_{38}N_2O_5S_1$ density 1.15 g cm^{-3} and melting point 89.1±0.5°C. The formula, density and melting point of PEG 6000 are $HOCH_2(CH_2OCH_2)_nCH_2OH$, 1.07 g cm^{-3} and 62.7±0.7°C, respectively [4]. The binary system has an eutectic point of composition 80 wt% PEG 6000 and an eutectic temperature of T_E=59±0.5°C. The aim of the present work is to study the thermodynamics and kinetics of the solidification process of the binary system of PEG 6000 and SR 33557 by

*Corresponding author. Tel.: 343 402 1182; fax: 343 402 1198; e-mail: narcis@ecm.ub.es.

PII S0040-6031(96)03077-8

differential scanning calorimetry (DSC). This technique is very useful and, as will be seen later, may provide useful knowledge on the solidification behaviour of blends of PEG and drugs if care is taken while interpreting the data [5].

2. Experimental

The experiments were performed on a Mettler DSC30 equipment. The instrument was calibrated for enthalpy and temperature using indium as standard. Mixtures of SR 33557 and PEG 6000 at various compositions were subjected to several thermal treatments to investigate their solidification kinetics. Experiments were performed under three conditions: constant heating rate, isothermally and constant cooling rates. Constant heating-rate experiments were performed, on an initially powdered mixture of the solid constituents, at 20 K min^{-1} up to the liquid state. Constant cooling-rate experiments were performed from the (assumed) isotropic melt state at rates ranging from 2.5 to 70 K min^{-1} down to −20°C. Isothermal experiments were performed by cooling the sample at 20 K min^{-1} from 10°C above melting point of the pure SR33557 drug (expected isotropic melt state) to a pre-determined value, where the crystallization process was monitored as a function of time.

3. Results and discussion

3.1. Thermodynamic study

Fig. 1 shows a sequence of scans obtained, at a heating rate of 20 K min^{-1}, for the initial mixtures of different compositions. The values obtained for the eutectic, T_E, and liquidus, T_L, temperatures are in agreement with previously published results [1]. The experimental values of the melting enthalpy per unit mass, ΔH_f, of some representative mixtures are reported in Table 1. There is a continuous decrease of ΔH_f with decrease in the PEG 6000 content.

The analysis of the results presented in Table 1 was carried out by neglecting the heat-capacity difference between the liquid and solid constituents. Then the melting enthalpy of a mixture may be written as

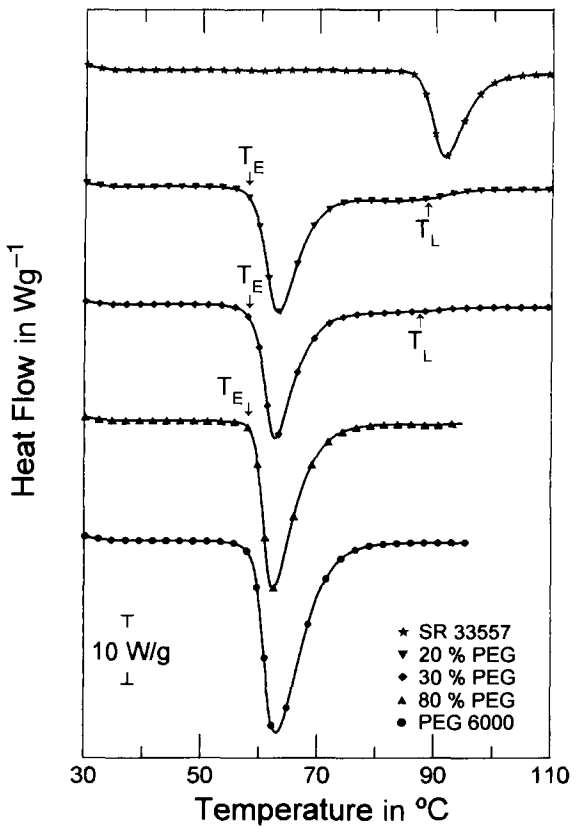

Fig. 1. DSC curves obtained on heating the initial mixtures of different compositions of the elemental constituents: T_E, eutectic temperature and T_L, liquidus temperature. Heating rate-20 K min^{-1}.

Table 1
Melting enthalpy. ΔH_f, of mixtures of the system SR 33557/PEG 6000. Average melting enthalpy, $\langle \Delta H_f \rangle$, of the constituents, and estimated contribution ot the mixing enthalpy, ΔH_{mix}

wt% PEG	100	80	30	20	0
ΔH_f (J/g)	199±10	158±8	146±8	120±8	75±6
$\langle \Delta H_f \rangle$(J/g)	—	174±8		112±8	100±8
ΔH_{mix} (J/g)	—	−16±16	34±16	20±16	—

$$\Delta H_f = H^{liq} - w_A H_A^{sol} - w_B H_B^{sol} = \Delta H_{mix} + \langle \Delta H_f \rangle, \quad (1)$$

where H^{liq} is the enthalpy of the liquid solution of composition w_A and w_B (weight fraction), H_C^{sol} (C=A,B) is the enthalpy of each constituent C in the solid state, ΔH_{mix} is the mixing enthalpy of the

liquid alloy and $\langle \Delta H_f \rangle$ is the average melting enthalpy of the mixture. That is,

$$\langle \Delta H_f \rangle = w_A \Delta H_f^A + w_B \Delta_f^B, \quad (2)$$

where ΔH_f^C is the melting enthalpy of constituent C.

The estimated value of ΔH_{mix} is presented in Table 1. The low absolute values obtained for this quantity suggest that the system showed a small deviation from the ideal behaviour.

The Gibbs mixing energy of the liquid solution (ΔG_{mix})

$$\Delta G_{mix} = \Delta H_{mix} - T\Delta S_{mix} \quad (3)$$

is expressed by the Flory–Huggins model [6,7] with the mixing enthalpy (ΔH_{mix}) and entropy per unit mass (ΔS_{mix}) given, respectively, by:

$$\Delta H_{mix} = \chi_A (w_A/P_{MA})\phi_B = \chi_B (w_B/P_{MB})\phi_A \quad (4)$$

$$\Delta S_{mix} = -R[(w_A/P_{MA})\ln\phi_A + (w_B/P_{MB})\ln\phi_B] \quad (5)$$

with χ_A (or χ_B) the interaction energy per volume fraction of B, ϕ_B (or of A, ϕ_A). The volume fraction of constituent C (C=A, B), ϕ_C, is given by

$$\phi_C = v_C(w_C/P_{MC})/[v_A(w_A/P_{MA}) + v_B(w_B/P_{MB})], \quad (6)$$

where P_{MC} is the molecular weight of C.

The phase diagram (Fig. 2) has been assessed while neglecting any miscibility in the solid state between the constituents. The optimized value obtained for the interaction energy is $\chi_A/P_{MA} = -2.18\ J\ g^{-1}$. With this interaction energy, the thermal energy per unit mass evaluated for SR 33557 at temperatures close to the eutectic is about $5\ J\ g^{-1}$, whereas the computed value is $\approx 0.5\ J\ g^{-1}$ for PEG 6000. Thus, comparison between these quantities confirms that the interaction between the constituents in the liquid solution is not negligible [1].

It is interesting to note the anomalous decrease of the liquidus temperature obtained experimentally at low drug concentration, as shown in Fig. 2. As reported elsewhere [5], this is a common feature of phase diagrams of PEG and drugs obtained by DSC, because the melting behaviour of a drug in a pool of molten PEG may not be the same as that of a pure drug.

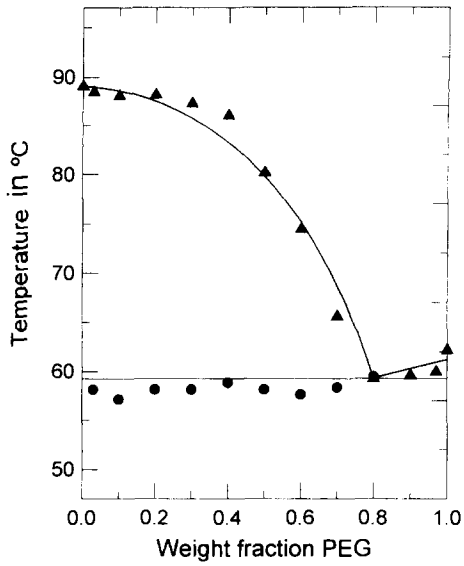

Fig. 2. The phase diagram of the system SR 33557/PEG 6000: ▲ liquidus temperature; • eutectic temperature. Continuous curve: calculated values.

3.2. Kinetic study

The kinetic study has been performed measuring the DSC signal either under constant cooling rate or on isothermal regime. Fig. 3 shows some of the scans corresponding to different compositions on cooling at $10\ K\ min^{-1}$. Both PEG 6000 and the 80 wt% PEG blend crystallized on cooling, but only partial crystallization occurred for the mixture containing 20% PEG. No crystallization was observed for SR 33557. A glass transition was observed for the latter two compositions (Fig. 4). That is, on cooling at $10\ K\ min^{-1}$, partial crystallization of the blend containing 20% PEG ended at about 5°C and the remaining undercooled liquid turned into glass below $T_g \approx -30$°C. SR 33557 remained in the undercooled state down to about 20°C.

To proceed to the analysis of the solidification under non-equilibrium conditions, we recall that under isothermal conditions, crystallization–kinetics analysis may be based on Avrami's equation

$$x = 1 - \exp - [(kt)^n], \quad (7)$$

where x is the degree of crystallinity, k the crystallization rate-constant, t the time and n a kinetic

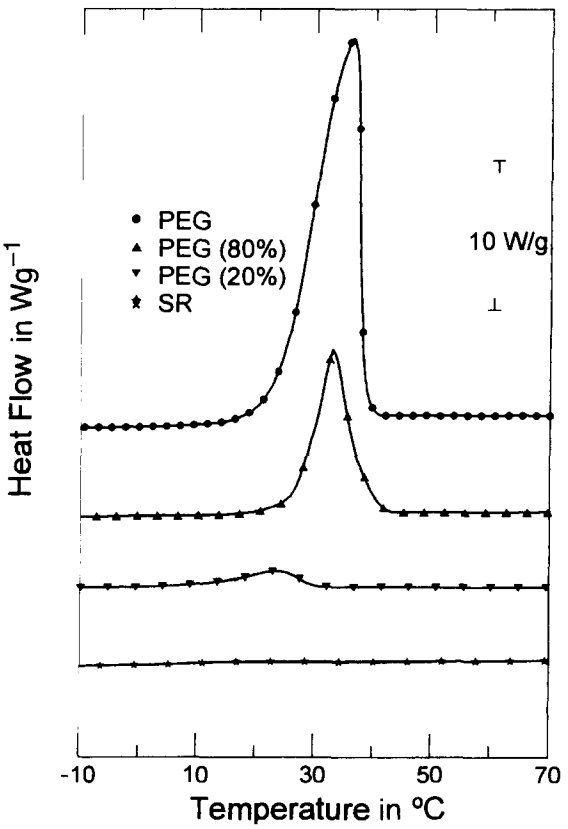

Fig. 3. DSC cooling curves for different compositions; cooling rate=10 K min^{-1}.

exponent which depends on the mechanism of crystallization. Table 2 lists the respective values of k and n for various model crystallization processes [8].

The direct derivative of Eq. (7) is

$$\frac{dx}{dt} = kf(x) \tag{8}$$

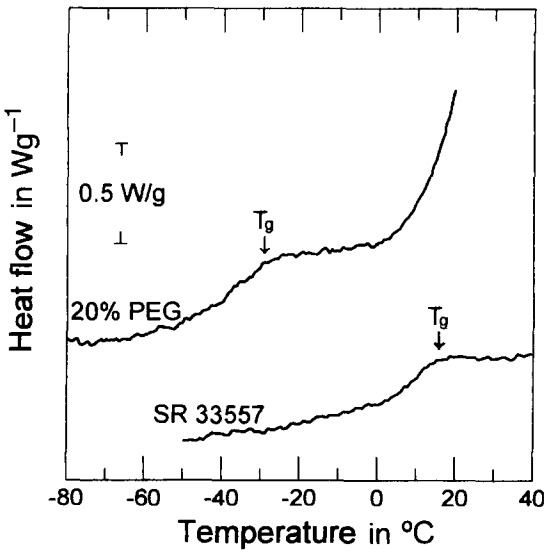

Fig. 4. Glass-transition range obtained in the DSC cooling curves shown in Fig. 3.

with

$$f(x) = n(1-x)[-\ln(1-x)]^{(n-1)/n}. \tag{9}$$

The same derivative under a continuous cooling (or heating) treatment at a constant rate β, sometimes referred to as the additivity assumption [9,10] but initially introduced by Doyle [11] to derive kinetic data from a thermogravimetric curve, is

$$\frac{dx}{dT} = \frac{kf(x)}{\beta}. \tag{10}$$

In the temperature range in which crystallization can be investigated by DSC, the crystallization rate-constant is generally assumed to follow the Arrhenius

Table 2
Avrami rate constant, k, and kinetic exponent, n, for various crystallization processes

Morphology of the crystalline grains	Pre-existing nuclei N_I : density of nuclei		Nucleation I : Nucleation frequency	
	k	n	k	n
One-dimensional growth : fibers of section S	$SN_I{}^{u\,a}$	1	$\left(\frac{SIu}{2}\right)^{1/2}$	2
Two-dimensional growth : rods of thickness L	$(\pi N_I L)^{1/2}u$	2	$\left(\frac{\pi LIu^2}{3}\right)^{1/3}$	3
Three-dimensional growth : spheres	$\left(\frac{4\pi N_I}{3}\right)^{1/3}u$	3	$\left(\frac{\pi Iu^3}{3}\right)^{1/4}$	4

[a] u: growth rate.

equation

$$k = A\exp(-E/RT), \tag{11}$$

where A is the pre-exponential factor and E the activation energy. There are various differential and integral methods to calculate these quantities from continuous heating data. In particular, the Kissinger method [12] assumes that

$$\frac{\mathrm{d}\ln(\beta/T_\mathrm{p}^2)}{\mathrm{d}(1/T_\mathrm{p})} = -E/R \tag{12}$$

where T_p is the peak maximum temperature, $(\mathrm{d}^2x/\mathrm{d}t^2)_{T=T_\mathrm{p}} = 0$ at a given rate β.

The Ozawa method [13] assumes that

$$\frac{\mathrm{d}\ln\beta}{\mathrm{d}(1/T_\mathrm{p})} = -E/R. \tag{13}$$

The values of E obtained in both the methods are similar [14,15].

From the values of E, and using Eqs. (8 and 10), it has been shown [16,17] that the predicted low temperature parts of the time–temperature (T–T–T) and temperature–heating rate (T–HR–T) transformation diagrams may be constructed from limited calorimetric data. However, no such prediction has been presented up to now for the construction of the temperature–cooling rate transformation (T–CR–T) diagrams [18].

In the modelling of the crystallization process, we will distinguish cold crystallization, for which the analysis mentioned above is often performed, as against solidification from the melt. Our purpose is to show that a very similar procedure can be used to analyze solidification data. The main difference is that cold crystallization of a polymeric mixture may be promoted by pre-existing nuclei. However, solidification from the isotropic melt is expected to be driven by nucleation.

It has long been recognized that a certain amount of undercooling $\Delta T = T_\mathrm{f} - T$, with T_f the melting temperature, is necessary to start solidification [19] because nuclei have to be created prior to any crystal growth. The driving force for nucleation is the Gibbs energy difference between the liquid and the crystal, ΔG, which at low undercooling is proportional to ΔT : $\Delta G \approx \Delta S_f \cdot \Delta T$, with ΔS_f the melting entropy [16]. However, an interfacial energy, σ, is necessary to form the interface between the liquid and the nucleus. As a consequence, the size of the fluctuating forming nucleus has to be larger than a critical size to be able to grow. As shown in Table 2, irrespective of the mode of growth, nucleation is activated by a crystallization rate-constant, k, which is proportional to some power of the nucleation frequency. The activation energy for homogeneous nucleation is of the form [16,20]

$$E_1 = \frac{16\pi\sigma^3}{(\Delta G)^2}. \tag{14}$$

Therefore, at low undercooling, one expects a rate-constant of the approximate form

$$k(T) = A'\exp[-B/T(\Delta T)^2], \tag{15}$$

where A' is a function of temperature, with a slower variation than the exponential factor in a temperature interval of $\Delta T \lesssim 0.2\,T_\mathrm{f}$ and B is a constant proportional to $\sigma^3/\Delta S_\mathrm{f}^2$.

Using that expression, the integral from Eq. (8) under isothermal regime at temperature T_0 up to a degree of crystallinity x_0 (annealing time t_0) is

$$g(x_0) = \int_0^{x_0} \frac{\mathrm{d}x}{A'f(x)} = \exp\left[-B/T_0(\Delta T_0)^2\right] \cdot t_0 \tag{16}$$

with $\Delta T_0 = T_\mathrm{f} - T_0$.

Similarly, under continuous cooling at a rate β_{C_0}, the integrated form of Eq. (10) becomes

$$g(x_0) = \int_0^{x_0} \frac{\mathrm{d}x}{A'f(x)} = \int_0^{\Delta T_0} \exp\left[-B/T(\Delta T)^2\right] \frac{\mathrm{d}(\Delta T)}{\beta_{C_0}}. \tag{17}$$

The quantity $g(x_0)$ is independent of the mode of crystallization, i.e. isothermal conditions or continuous cooling conditions. Once its value for a given crystalline fraction x_0 is known, the analytical expression for $x_0 = x_0(T,t)$ for any pair (T,t) is given by

$$\exp\left[-B/T(\Delta T_0)^2\right] t_0 = \exp\left[-B/T(\Delta T)^2\right] \cdot t \tag{18}$$

and the analytical expression of $x_0 = x_0(T, \beta_\mathrm{C})$ for any

pair (T,β_C) is given by

$$\int_0^{\Delta T} \exp\left[-B/T(\Delta T)^2\right] \frac{d(\Delta T)}{\beta_C} = \int_0^{\Delta T_0} \exp\left[-B/T(\Delta T)^2\right] \frac{d(\Delta T)}{\beta_{C_0}}. \quad (19)$$

Thus, the forms of the curves $T=T(t)$ and $T=T(\beta_C)$, for a fixed value of x, are obtained by means of Eqs. (18 and 19) provided the values of T_f and B are known.

In the present study the values of the melting temperature T_f and of the constant B have been obtained from the best fit approach to the experimental data under a constant cooling rate. The value of B is

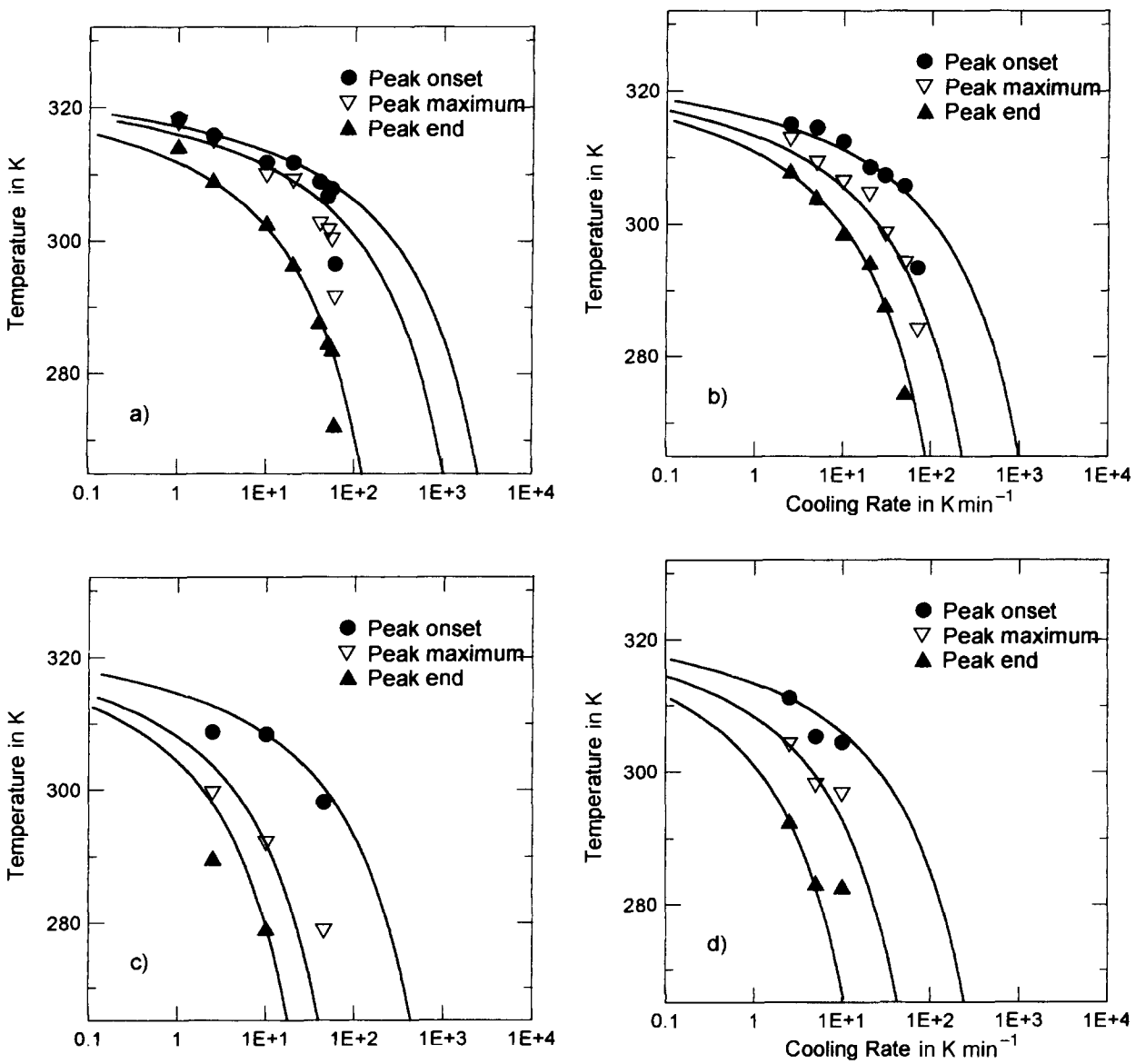

Fig. 5. T–CR–T curves obtained for the following compositions: (a) PEG 6000; (b) 80 wt% PEG; (c) 30 wt% PEG; (d) 20 wt% PEG. Experimental • onset, ▽ maximum and ▲ end peak temperatures. Continuous curves: calculated values.

determined by a procedure similar to the Kissinger method, that is by imposing $(d_2x/dt^2)_{T=T_p} = 0$ at a given cooling rate β. The approximate value of B is

$$\frac{d\ln\left[\beta(3T_p - T_f)/T_p^2(T_f - T_p)^3\right]}{d(1/[T_p(T_f - T_p)^2])} \approx -B. \quad (20)$$

There is some scatter in the values obtained for each mixture when applying Eq. (20), which is deduced by taking T_f=332 K. The value of B is:

$$B = 33.8 \times 10^4\ K^{-3}. \quad (21)$$

Figs. 5 and 6 show the result of the analysis performed for crystallized fractions x_0 corresponding to

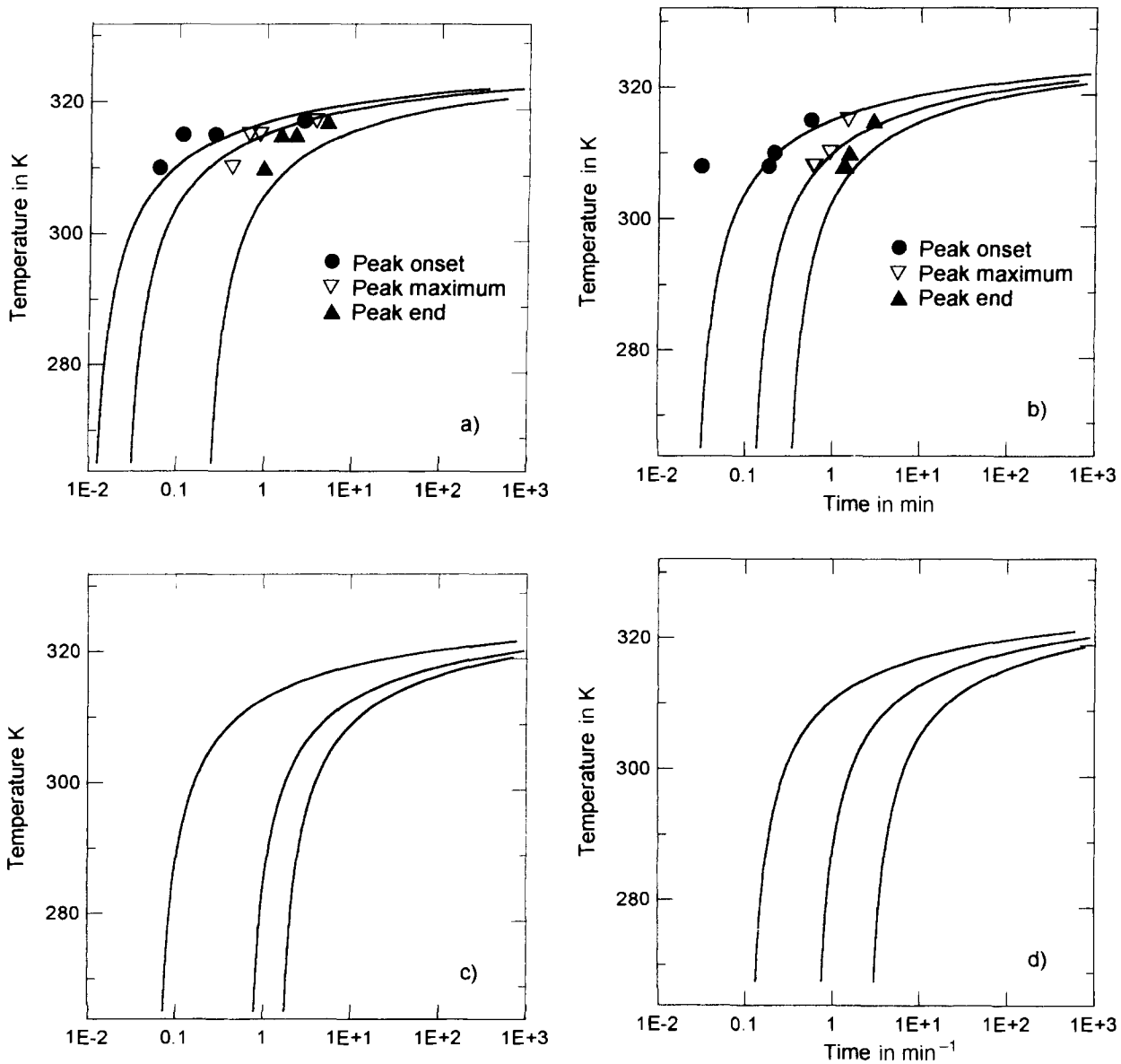

Fig. 6. T–T–T curves obtained for the following compositions: (a) PEG 6000; (b) 80 wt% PEG; (c) 30 wt% PEG; (d) 20 wt% PEG. Experimental • onset, ▽ maximum and ▲ end peak temperatures. Continuous curves: calculated values.

the onset, maximum and end of the peak temperatures. The respective calculated pairs (T,t) and (T,β_C) are presented in the form of continuous curves in T–CR–T and T–T–T transformation diagrams, respectively. The experimental data, shown as discrete points, show some scatter which is representative of the quality of reproducibility of the experimental behaviour. As expected in a solidification process, the onset of crystallization shifts to higher temperatures on decreasing the cooling rate and to longer times on decreasing the annealing temperature under continuous cooling and isothermal regimes, respectively. With respect to the calculated curves, in all the diagrams the same values of T_f and B, given in Eq. (20), are used. The good agreement, shown in Fig. 6, between the predicted T–T–T curves and the experimental data (for two compositions) confirms that a unified picture may be presented in order to account for the solidification behaviour under non-equilibrium conditions. Another point to be stressed is the significant decrease of the temperature of solidification with cooling rate (under continuous cooling) or with time (under isothermal treatment) with decreasing PEG 6000 content. This fact evidences the increasing glass-forming ability of the melt with decreasing PEG content and agrees with the experimental behaviour.

4. Conclusions

Several mixtures of SR 33557 and PEG 6000 were subjected to different thermal treatments to investigate the thermodynamics and kinetics of the solidification process. The temperatures of transformation and enthalpy changes have been measured by means of differential scanning calorimetry. A negative interaction energy between the constituents accounts for the experimental phase diagram data and is in agreement with the measured melting enthalpy of the alloys. Solidification from the melt is presented in a unified picture accounting for isothermal as well as continuous cooling regime. The analysis is based on the fact that nuclei have to appear prior to any crystal growth. The high temperature part ($\Delta T \lesssim 0.2\,T_f$) of both the T–T–T and the T–CR–T diagrams were constructed over a wide range of conditions.

Acknowledgements

Support from the Comissió Interdepartamental de Recerca i Tecnologia (CIRIT) by Projects No. AIRE92-4 and GRQ-2.048 is acknowledged.

References

[1] J. Lheritier, A. Chauvet and J. Masse, Thermochim. Acta 241 (1994) 157.
[2] P. Nokin, M. Clinet and P. Polster, Arch. Pharmacol 339 (1989) 31.
[3] C. Lacour, F. Canals, G. Galindo, P. Chatelain and D. Nisato, Arch. Mal. Coeur. 83 (1990) 1281.
[4] J. Lheritier, Thesis, Université de Montpellier (1995).
[5] D.Q.M. Craig, Thermochim. Acta 248 (1995) 189.
[6] P.J. Flory, J. Chem. Phys. 10 (1942) 51.
[7] M.L. Huggins, J. Am. Chem. Soc. 64 (1942) 1712.
[8] T. Hatakeyama and F.X. Quinn, Thermal Analysis, Fundamentals and applications to Polymer Science, Wiley, New York (1995).
[9] D.R. MacFarlane, J. Non-Cryst. Solids 53 (1982) 61.
[10] D. Dollimore, T.A. Evans, Y.F. Lee and F.W. Wilburg, Thermochim. Acta 188 (1991) 77.
[11] C.D. Doyle, J. Appl. Polymer Sci. 5 (1961) 285.
[12] H.E. Kissinger, Anal. Chem. 29 (1957) 1702.
[13] T. Ozawa, Bull. Chem. Soc. Japan 38 (1965) 1881.
[14] J. Sestak, Phys. Chem. Glasses 15 (1974) 137.
[15] D.W. Henderson, J. Non-Cryst. Solids 30 (1979) 301.
[16] N. Clavaguera, J. Non-Cryst. Solids 162 (1993) 40.
[17] N. Clavaguera and M.T. Clavaguera-Mora, Mat. Sci. Eng. A179-A180 (1994) 288.
[18] M.T. Clavaguera-Mora, S. Surinach, M.D. Baró and N. Clavaguera, Solid State Ionics 63-65 (1993) 68.
[19] D. Turnbull, Contemp. Phys. 10 (1969) 473.
[20] D.R. Ulhmann, J. Non-Cryst. Solids 7 (1972) 337.